Nuclear Engineering and Technology 54 (2022) 4338–4347

Contents lists available at ScienceDirect

Nuclear Engineering and Technology

journal homepage: www.elsevier.com/locate/net

Original Article

Benchmarking of the CUPID code to the ASSERT code in a CANDU channel

Eun Hyun Ryu [a, *], Joo Hwan Park [b], Yun Je Cho [a], Dong Hun Lee [c], Jong Yeob Jung [a]

[a] Korea Atomic Energy Research Institute, 989-111, Daedeok-daero, Yuseong-gu, Daejon, South Korea
[b] Nuclear Engineering Service & Solution, 6, jibhyeonjungang 7-ro, Sejong, South Korea
[c] Korea Institute of Nuclear Safety, 62, Gwahak-ro, Yuseong-gu, Daejeon, South Korea

ARTICLE INFO

Article history:
Received 20 December 2021
Received in revised form
25 May 2022
Accepted 29 June 2022
Available online 5 July 2022

Keywords:
CUPID
V&V
PHWR
ASSERT
Sub-channel level

ABSTRACT

The CUPID code was developed and is continuously updated in KAERI. Verification and validation (V&V) is mainly done for light water reactors (LWRs). This paper describes a benchmarking of the detailed mesh level compared with sub-channel level for application to pressurized heavy water reactors (PHWRs), even though component scale comparison for the PHWR moderator system was done once before. We completed a sub-channel level comparison between the CUPID code and the ASSERT code and a CUPID code analysis. Because the ASSERT code has already been validated with numerous experiments, benchmarking with the ASSERT code will offer us more trust on the CUPID code. The target channel has high power and thus high pressure deformation. The high power channel tends to have a high possibility of critical heat flux (CHF), because a high void fraction and quality in channel exit region appear. In this research, after determining the reference grid and T/H model, we compared the sub-channel level results of the CUPID code with those of the ASSERT code.

1. Introduction

1.1. Used codes

The ASSERT code was developed at Chalk River Laboratories (CRL) to simulate transient single- and two-phase flows for axial and radial directions and heat transfer in rod-bundle fuel channels in the CANDU 6 reactor [1]. The drift-flux model (unequal velocity/unequal temperature) was used and a two-dimensional code. Because the ASSERT code has been well verified and validated with various codes and experiments, this benchmarking with the ASSERT code can be a step for verification and validation of the CUPID code in a CANDU6 channel analysis [2] although ultimate full and complete validation should have gone for more number of experiments and cases.

The CUPID code was developed at the Korea Atomic Energy Research Institute (KAERI) to compute two-phase multi scale T/H calculations [3,4]. Although it has been verified and validated with many codes and experiments for a broad range of scales (from a CFD scale to a system scale-it is an ultimate goal of the CUPID code, which can be used all T/H analysis independent of the scale), all such studies were for light water reactors, though a few benchmarking studies for a CANDU6 moderator system have been done but with a porous medium approach and almost single phase analysis [5,6]. The CANDU6 channel condition presents a difficult problem for the CUPID code because there are heating conditions with boiling and so two-phase simulation is needed. In addition, the complexity of the CANDU6 geometry is a major factor for unstable calculation. Although we already have the ASSERT code for the CANDU6 type channel analysis, the ASSERT code has a limitation on the geometry change such as pressure tube sagging and ballooning. To precisely analyze the thermal margin decrease in the CANDU6 type channel due to the pressure tube deformation as reactor ages, a code which have capability to capture unstructured geometry. Because the CUPID code is using Finite Volume Method (FVM) and well verified and validated for the PWR, the FVM methodology will operate correctly even for the CANDU6 type core. By the way, the CUPID code is not using the Boussinesq approximation in this study because that the forced convection is dominated phenomenon in this problem. It was turned out that the difference between using the steam table and the Boussinesq approximation is negligible for the natural convection [7].

* Corresponding author. Korea Atomic Energy Research Institute, 989-111, Daedeok-daero, Yuseong-gu, Daejon, 34057, South Korea.
E-mail address: ryueh@kaeri.re.kr (E.H. Ryu).

https://doi.org/10.1016/j.net.2022.06.030

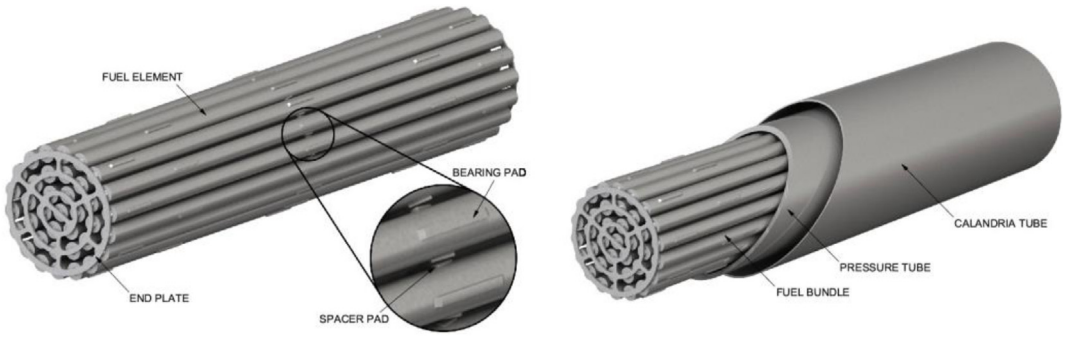

Fig. 1. (a) A 37 element CANDU fuel bundle, and (b) the configuration of a CANDU fuel channel [14].

Governing equations used in the CUPID code can be found in the CUPID manual [8].

1.2. Recent related researches and research object

Tries to find the actual flow behavior in the CANDU6 channel have been done many times, specially with respect to the pressure tube aging issue in the CANDU6 channel. Piro and et al. [9] tried to reproduce detailed flow distribution based on the experiment for the fresh pressure tube. But despite of its speciality on CFD simulation, heating condition is missed in the contents. Zheng analyzed flow distribution inside of fresh and aged pressure tube [10]. But it is also lack of conditions to simulate real channel in aspects of heating condition and single phase. Importance of flow distribution inside of fresh fuel arises because that it is start of precise analysis of aged pressure tube. During the operation, pressure tube suffers from geometrical deformation, it causes decrease in safety margin. Ultimately, this research will be used and be expanded further to incorporate the reactor physics feedback, additional pressure tube deformation phenomenon and heating condition which will make the study much close to the real channel. The crucial motivation on pressure aging study is reported by Lee and et al. [11].

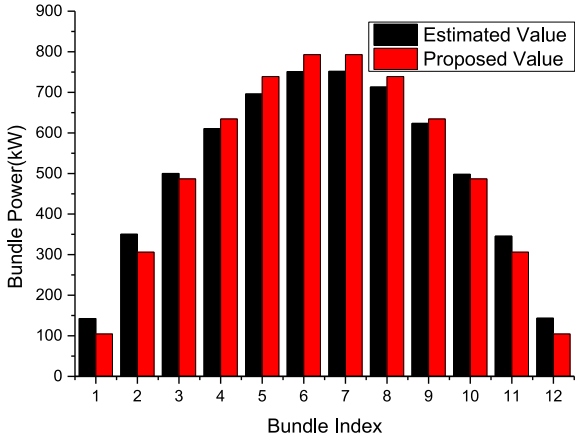

Fig. 2. Estimated and proposed axial powers.

1.3. CANDU6 specific features

CANDU6 has its own characteristics for several aspects which are much different from those of the LWR. The flow direction is horizontal and thus the gas and liquid velocity profiles are different from those of a vertical channel such as in the LWR assembly. The CANDU6 allows boiling inside of the heated section so that two phases coexist inside the channel. Because of different channel flow rates and powers, each channel has its own figures of merit, for example, the void fractions of the channels are much different from each other while the void fractions of all the assemblies in the LWR are zero. Due to the complexity of the channel geometry as shown in Fig. 1, unlike the PWR situation, each fuel rod doesn't have same surrounding coolant volume. In addition, pin power is different for each fuel array. Flow rate for each sub-channel is different from each other. These CANDU6 specific features need to be well reflected in the CUPID benchmarking.

1.4. T/H in a CANDU channel

In this study, we selected a high power channel along with the flow rate data, critical power ratio (CPR) will be much lower compared with low power channel-much lower thermal margin compared with that of low power channel. In addition, a clear two-phase can be observed in a high power channel in general. In fact, most dangerous-it means high chance to go through CHF-bundle is not 12-th bundle which locates in channel exit but bundle-most cases, among 8–10 bundle-where two-phase state develops fast. Narrow coolant region around the center rod is major factor including other reasons such as fuel sagging on spatial enthalpy and void imbalances which appear in the radial direction. Many appendages are attached in real CANDU reactors to maintain distance from one rod to another (space grid) or from rod to pressure tube (bearing par). In addition to their original purpose, they cause mixing effect as obstacle so that they contribute to reduce the energy imbalance. But simulating all those components in heated

Table 1
Ring power distribution for the average bundle discharge burnup (160 Wh/kg (U)).

Element Ring	Number of Elements	Element Power		Percent Power	
		Nor. To Bundle Avg.	Nor. To Outer Element	Per Element	Per Ring
Outer	18	1.120	1.000	**3.026**	54.46
Intermediate	12	0.9254	0.8266	**2.501**	30.01
Inner	6	0.8247	0.7367	**2.229**	13.37
Center	1	0.7843	0.7006	**2.120**	2.120

Table 2
T/H values for the coolant region.

	Initial Value	Inlet Condition	Outlet Condition
Pressure (Pa)	11.4E6		10.0E6
Liquid Temperature (K)	535.61		N/A
Void Fraction	0.0		N/A
NCG Quality	0.0		0.0
Velocity (m/s)	8.3229		N/A

conditions and two-phase conditions impose a tremendous amount of work for modeling and analysis. To focus on flow prediction, we omitted the appendages such as the end plate, space grid and so on in the simulations that we performed with the CUPID and the ASSERT Code. Although, 37 M fuel is decided to be used in the Wolsong unit 2,3 and 4 because of thermal margin, the 37 standard fuel is analyzed in this study.

From the point of view of CHF, it is well known that the quality, pressure and mass flux are major factors. Thus in this study, 3 quantities were mainly compared with the ASSERT code. In addition to those three factors, the fluid temperature and density were compared as well for the future reactor physics coupled simulations. Although 8–10 bundles have more importance compared with the other bundles from the CHF point of view, we compared the above mentioned parameters in the 12-th bundle as well. Because the values in the channel exit are reference values before entering headers, for example, quality is the maximum at the channel exit, it will continuously decrease along with the feed pipe because there is no heat source there.

2. Modeling of problem

2.1. Heat loss and boundary conditions

Among 380 channels in the core, we chose only the channel that was expected to have the most severe deformation for the analysis. Although we had many structures, such as the fuel, coolant, pressure tube, gap, calandria tube, we modeled only the fuel elements and coolant in the simulation because we found that the heat transfers through the radial direction such as radial conduction in a pressure tube or a calandria tube, convection heat transfer in CO_2 gap tube were almost negligible as was the axial solid heat conduction. Note that heat transfer modes of convection and conduction are used in the CUPID simulation. Due to this observation-quantitative analysis with modeling which incorporates gas gap, calandria tube and constant temperature boundary condition for calandria tube outer surface was done prior to this study, a result showed that the radial heat loss and heat transport by CO_2 gas are 4.9% and 1.5%, respectively, we set the radial outer surface of pressure tube to adiabatic boundary conditions as well as the fuel element top and bottom surfaces. Of course the coolant inlet and pressure boundary conditions were set respectively at the corresponding surfaces.

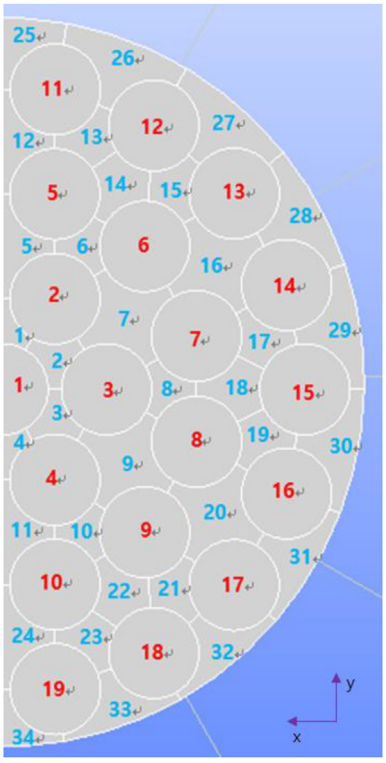

Fig. 3. Sub-channel and rod indexing (inlet view).

2.2. Channel selection and power profile

Because only the channel (Wolsong Unit 1, Q7) that had the most severe pressure tube deformation was selected based on the regular detector data, the power of the selected channel was known through the time-average calculation of the RFSP-reactor physics code of the CANADA-code. The total channel power was about 6127 kW and the power distribution was assumed as having a cosine shape even though the actual shape was somewhat different from the predetermined cosine shape, we expected that it would not cause a big difference, as Fig. 2. The ring power distribution is shown in Table 1 from the mid-burnup point. The T/H conditions are summarized in Table 2. The initial fuel temperatures were set to the same as an initial temperature of 535.61 K to prevent unstable code running from the impact of the temperature difference.

2.3. Appendages and pressure drop

As shown in Fig. 1, attachments such as the end plate, bearing pad, and element spacers exist in a bundle. These attachments have their own purposes, for example, spacers maintain the original design distance from one fuel element to another, and they cause a pressure drop. Those attachments take almost 70% of the pressure

Table 3
Important dimensions and other specifications.

Region Boundary	Dimension (cm) or Specification	Reference/CUPID Material	Reference/CUPID Initial Temperature (K)
Fuel Radius	0.64808	UO_2, He, Zr4/UO_2+He + Zr4 Volume Weighted	960.15/535.61
Pressure Tube Inside Radius	5.1689	D_2O(99% purity)/D_2O only	561.15/535.61
Pressure Tube Outside Radius	5.6032	Zr–Nb/Stainless Steel	561.15/342.15
Calandria Tube Inside Radius	6.4478	CO_2/Air	451.65/451.65
Calandria Tube Outside Radius	6.5875	Zr-2/Stainless Steel	342.15/342.15
Bundle Length	49.53	N/A	N/A
Number of Bundles	12	N/A	N/A

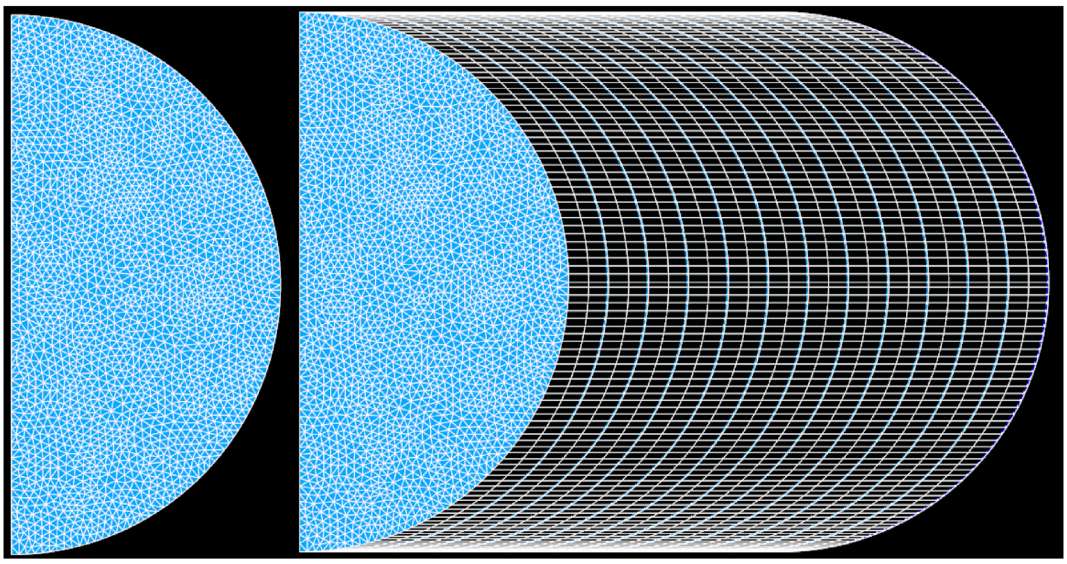

Fig. 4. (a) A cross section of the reference case and (b) the axial view of the reference case.

Table 4
Thermal Conductivity before/after Volume Weighting of Fuel Region.

Region Name		Pellet	Gap	Cladding	Merged Material
Volume Fraction		0.88	0.03	0.09	1.00
Material		UO_2	He	Zr	UO_2+He + Zr
Temperature (K)		Thermal Conductivity (w/mK)			
1	273.15	7.3	0.151	13.6	7.7
2	373.15	7.3		14.1	7.7
3	473.15	6.7		14.8	7.2
4	573.15	5.8		15.8	6.6
5	673.14	5.1		16.9	6.1
6	773.15	4.6		18.1	5.7
7	873.15	4.2		19.5	5.5
8	973.15	3.8		21.1	5.3
9	1073.15	3.5		22.8	5.2
10	1173.15	3.3		24.6	5.1
11	1273.15	3.1		26.8	5.2
12	1373.15	2.9		29.2	5.2
13	1473.15	2.8		31.7	5.3
14	1573.15	2.6		34.4	5.5
15	1673.15	2.5		37.3	5.6
16	1773.15	2.5		40.4	5.9

drop among a nearly 1Mpa pressure drop which occurs in a typical high power CANDU6 channel while rest of the pressure drop is due to the wall friction. Though we have now some distance from real reactor simulation because of the decreased pressure drop by omitting appendages in the modeling stage, modeling work and calculation time decreased considerably. Although, there are different purposes of appendages, eventually appendages will contribute to increase the pressure drop and mixing effect. Thus, eliminating them from the channel will cause more void and spatial imbalances through the channel. It was verified that about 20% more void appeared in w/o appendage case compared with appendage case in sub-channel 1 of bundle 12-exit bundle. Nevertheless, we are still holding critical circumstances such as heating condition and two phase flow. In the future, CUPID analysis with detailed appendage modeling should be proceed.

2.4. Important dimensions and fuel sagging

We took important dimensions such as fuel radius, pressure tube radius, calandria tube radius and so on, from known information for the Wolsong unit 1 as shown in Table 3. As interesting fact of CANDU 6 is that the fuel is already sagged as it is loaded in the channel because of gravity and its own weight. Conventionally, the value of eccentricity was set as 0.7828 mm, less than 1 mm. Depend on the bearing pad shape, circumstance and pressure tube radius, the value can vary. To have conservative approach, a value of 1 mm eccentricity is used in this study, which is slight high compared with conventional value. This fact is reflected in the modeling step as shown in Fig. 3. The region index can also be found in Fig. 3 as well. We prepared it so that both the CUPID and the ASSERT code region indexes were consistent from code to code.

2.5. Symmetric boundary condition at the center, fuel region integration and pressure-velocity coupling

It was reported that there are big differences between the velocities of gas and liquid for a horizontal flow channel [12]. When the difference between the velocities of the two phases exceeds a

Table 5
Heat Capacity before/after Volume Weighting of Fuel Region.

Region Name		Pellet	Gap	Cladding	Merged Material
Volume Fraction		0.88	0.03	0.09	1.00
Material		UO_2	He	Zr	UO_2+He + Zr
Temperature (K)		Heat Capacity (J/m^3K)			
1	273.15	2.43E+06	927.3	1.88E+06	2.306E+06
2	373.15	3.01E+06		2.08E+06	2.838E+06
3	473.15	3.17E+06		2.21E+06	2.987E+06
4	573.15	3.24E+06		2.29E+06	3.055E+06
5	673.14	3.24E+06		2.38E+06	3.070E+06
6	773.15	3.31E+06		2.38E+06	3.124E+06
7	873.15	3.31E+06		3.63E+06	3.245E+06
8	973.15	3.32E+06		4.46E+06	3.327E+06
9	1073.15	3.33E+06		4.95E+06	3.379E+06
10	1173.15	3.34E+06		5.12E+06	3.401E+06
11	1273.15	3.34E+06		4.95E+06	3.393E+06
12	1373.15	3.35E+06		4.46E+06	3.354E+06
13	1473.15	3.35E+06		3.36E+06	3.256E+06
14	1573.15	3.36E+06		2.38E+06	3.174E+06
15	1673.15	4.12E+06		2.38E+06	3.841E+06

Table 6
Model choice for the reference case.

Turbulence	Interfacial Heat Transfer	Drag Force
K-epsilon model Two phase model	Bubbly and mist topology map Ranz and Marshall Interfacial heat transfer model	Ishii for drag force model Turbulent dispersion user value, 0.4 Lift force user value, 0.01 Wall lubrication force user value, 0.1

Table 7
Mesh data[a] for the sensitivity calculation.

Case		Explanation	Number of Nodes	Number of Volumes	Axial Length (cm)	Avg. Volume (cm^3)	Avg. Triangle Area (cm^2)
	Case 0	Base mesh size	20,550	36,840	24.77	0.68	0.027
Axial Refinement	a-1	Refined 0	30,414	55,260	16.51	0.45	0.027
	a-2	Refined 1	40,278	73,680	12.38	0.34	0.027
	a-3	Refined 2	50,142	92,100	9.91	0.27	0.027
Radial Refinement	r-1	Refined 0	32,625	59,232	24.77	0.42	0.017
	r-2	Refined 1	50,050	91,800	24.77	0.27	0.011
	r-3	Refined 2	78,425	145,272	24.77	0.17	0.007
	r-4	Refined 3	108,550	202,008	24.77	0.12	0.005
Global Refinement	g-1	Refined 0	48,285	88,848	16.51	0.28	0.017
	g-2	Refined 1	98,098	98,098	12.38	0.14	0.011
	g-3	Refined 2	191,357	191,357	9.91	0.07	0.007

[a] Domain Volume = 1/40 m^3, half of the pressure tube inside.

Table 8
Pressure drop and T/H results of bundle 12[a].

Case		Pressure Drop (kPa)	Equilibrium Quality Change[b] (%)	Avg. Equilibrium Quality (%)	Avg. Mixture Enthalpy (kj/kg)	Flow Area Rel. Error[b] (%)
	Case 0	232	N/A	−0.01	1350.4	3.74
Axial Refinement	a-1	244	0.08	−0.03	1350.5	3.74
	a-2	238	0.12	−0.02	1350.5	3.74
	a-3	242	0.15	−0.03	1350.4	3.74
Radial Refinement	r-1	240	0.69	0.14	1352.1	2.29
	r-2	250	0.92	0.26	1353.6	1.53
	r-3	255	0.85	0.34	1354.4	1.15
	r-4	258	0.98	0.36	1354.7	0.95
Global Refinement	g-1	252	0.69	0.12	1352.2	2.29
	g-2	256	1.00	0.24	1353.6	1.53
	g-3	267	0.91	0.30	1354.4	1.15

[a] References of the ASSERT Code: Avg. Equilibrium Quality (0.82%), Avg. Mixture Enthalpy (1361.5kj/kg), Flow Area(17.73 cm^2).
[b] Equilibrium Quality Change: Mass Weighted Root Mean Square Error (RMSE) compared with case 0.

Table 9
Sensitivity for the interfacial model in bundle 10.

Sub-channel Index	Sub-channel Area (m^2)	Equilibrium Quality		Mass Flux	
		Ref.	Difference (%)	Ref (kg/m^2s)	Relative Difference (%)
1	1.53E-05	8.9	−0.23	4.31E+03	1.03
2	3.05E-05	8.0	0.04	4.46E+03	−0.16
3	3.05E-05	6.7	−0.26	4.59E+03	1.01
4	1.53E-05	6.9	−0.06	4.22E+03	0.00
5	4.54E-05	−1.1	0.06	6.81E+03	−0.09
6	3.05E-05	3.7	−0.09	5.17E+03	0.56
7	9.04E-05	−1.9	0.03	7.06E+03	−0.06
8	3.15E-05	7.6	−0.07	4.67E+03	−0.24
9	9.07E-05	−2.1	0.03	7.11E+03	−0.09
10	3.05E-05	6.7	−0.16	4.71E+03	0.69
11	4.54E-05	−1.4	−0.04	6.95E+03	0.21
12	4.59E-05	0.0	0.00	6.89E+03	0.00
13	3.99E-05	1.4	0.04	6.54E+03	−0.23
14	5.02E-05	2.2	−0.01	6.24E+03	0.07
15	4.00E-05	1.2	0.02	6.71E+03	−0.23
16	9.04E-05	−0.1	0.00	7.01E+03	−0.05
17	3.98E-05	0.9	0.00	6.58E+03	−0.03
18	5.12E-05	−1.2	−0.03	7.35E+03	0.16
19	4.00E-05	1.9	0.06	6.39E+03	−0.50
20	9.19E-05	−0.6	−0.01	7.11E+03	0.08
21	4.00E-05	3.8	−0.02	5.72E+03	0.19
22	5.02E-05	−1.0	−0.01	7.49E+03	−0.02
23	3.99E-05	2.3	0.07	6.16E+03	−0.54
24	4.59E-05	0.1	0.00	6.90E+03	0.00
25	4.68E-05	−8.0	0.00	7.24E+03	−0.07
26	9.25E-05	−7.3	0.00	7.32E+03	−0.02
27	8.93E-05	−6.8	0.00	7.21E+03	0.00
28	8.44E-05	−7.3	0.00	7.20E+03	−0.07
29	7.84E-05	−6.1	0.00	6.94E+03	−0.07
30	7.22E-05	−4.4	−0.01	6.74E+03	−0.03
31	6.64E-05	−1.5	0.00	6.31E+03	0.10
32	6.17E-05	0.3	0.00	5.91E+03	−0.09
33	5.87E-05	2.0	−0.06	5.48E+03	0.40
34	2.88E-05	0.5	0.03	5.86E+03	−0.26
Sum.	1.80E-03	N/A	N/A	N/A	N/A
Avg.	5.29E-05	N/A	N/A	6.58E+03	N/A

certain limit, the stability of the CUPID code significantly drops. To give more stability in running the code and to have fast calculations, symmetric boundary condition is applied at the yz plane-note that the flow and gravitational force directions are aligned on the z-axis and y-axis, respectively. Even with conceptual symmetric conditions established, the experimental results were not symmetric and neither were the results of the ASSERT code. Due to the application of the symmetric boundary conditions to the CUPID code, a difference can occur between the two results. This difference is sometimes marginal and sometimes considerable. As shown in Table 3, region integration of pellet, gap and cladding in this study is a kind of compromise. Because we have 37 fuel rods in a bundle, there will be too much complexity in the modeling stage if we model all 37 fuel rods, their sagging and 3 sub-regions in a fuel rod. Even though we grant necessity of region integration, still there may be a question that volume averaging is the best way or not. But the volume averaging is most frequently used way-because it is generally gives reasonable solution on T/H problems and its effectiveness over other methods is not tested in this research. During this process, the conductivity and thermal capacity of UO_2, helium, and Zircaloy were averaged with volume weighting. Detailed thermal properties after volume weighting and those of raw material depend on temperature is shown in Table 4 and Table 5. Basically, the CUPID code took data from the MARS code. Because volume fraction of the gap region is extremely small, it is assumed that its property constant. In the CUPID code, user can choose among Implicit Continuous Eulerian (ICE), Simplified Marker and Cell (SMC) and decoupled method. In this study, by considering the stability and generality mass and energy conservation equations are both used for solving the pressure-ICE method is used. Due to the technical problem, it was difficult to use heat flux condition for fuel rod wall boundary condition. Moreover, to see the reactor physics feedback effect, solid temperature should be calculated. For these reason, the fuel region is modeled and meshed as well. However, in this thesis, the fuel temperature comparison is not reported because it is not main interest in flow distribution. Thus the conduction equation is solved in the solid region and it is coupled with fluid region in the CUPID simulation.

3. Reference case and sensitivity study items

A reference model-including reference mesh, turbulence model and input setting, all the details for the CUPID simulations-must be fixed and taking a look into branch cases will be better approach for this kind of problem. For representative model options for the reference case, we chose k-epsilon for the turbulence model. The Ishii interfacial drag force model was set as the reference model. Important option choices are listed in Table 6.

To determine the mesh sensitivity, we considered two directions. Two axial segments in a bundle were set for the reference while one axial segment increment was applied for the axially refined case. For the radial direction, the number of meshes between fuel rods was increased about 1.7 times for the radially refined case without change in the number of axial segments. We also prepared an additional case of the global refined case to observe the integrated effect. Thus, we had three categories to compare to examine the mesh directional sensitivity. For the drag

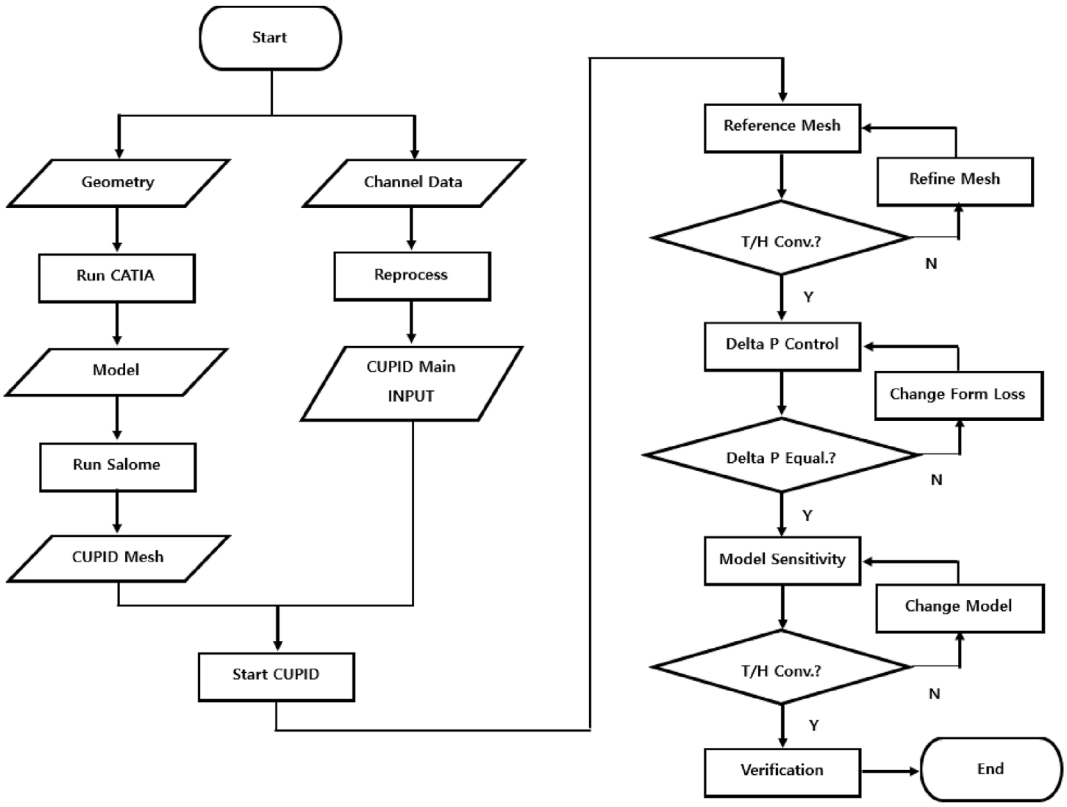

Fig. 5. Work flow.

force model, we tested two variations, Ishii model and the linear model.

4. Numerical results

Because of the difference between the default mesh sizes of the ASSERT code and the CUPID code, direct comparison was impossible. Thus, we used a collection of results of the CUPID code for a volume which matches the sub-channel of the ASSERT code. This kind of comparison is not uncommon as it frequently has been done for comparison results [13]. Most values were averaged by volume weighting while several parameters such as equilibrium quality and mixture enthalpy were averaged by mass weighting. Even though it is known that the most probable bundle number for the CHF is 10, the 12-bundle will have the biggest error because of continuous integration along with flow direction. For this reason, we compared parameters in 12-bundle for reference mesh determination.

While all the produced results are not shown in this paper, the pressure differences matched each other within 10 kPa (reference pressure drop without attachment was about 326 kPa from the ASSERT code calculation). Moreover, we observed the CANDU specific characteristics for all cases: namely, a slight drop of fluid temperature around bundle 9 because of a decrease in saturation temperature due to the pressure drop and solid and fluid temperature asymmetry on the flow direction, temperature, enthalpy and void increment around bottom of the pressure tube because of sagging and the center fuel rod.

4.1. Mesh sensitivity and reference mesh

Because the major parameters may vary according to the mesh size, we needed to extract a sufficiently converged result that had a physically understandable change with the mesh size. To choose the reference mesh size, a mesh size sensitivity study needed to be conducted prior to the other sensitivity studies. In Table 7 presents a total of eleven cases which include the base mesh size and ten refined cases as well as case names. Note that refinements for both the radial and axial directions are tested independently and along with a combination for both directions.

As shown in Table 8, the axial refinement had almost no impact on the listed T/H results (the equilibrium quality distribution, average equilibrium quality average mixture enthalpy and pressure drop). However, the radial refinement did affect the T/H results. By increasing the radial number of the mesh, all the listed results showed asymptotic behavior. At the same time, flow area goes to the original value. Thus, it is revealed that the globally refined results are the mere sum of the axial and radial results. Moreover, the global refinement results are almost the same as the radial refinement results.

When we examined the mesh sensitivity results, we decided that no more axial refinement was necessary because no new gains were expected. Case r-2 was selected as the reference case because it had converged sufficiently as shown in Table 8. Its mesh was shown in Fig. 4.

4.2. Interfacial momentum model sensitivity

In order to catch the variation in results depend on the momentum model, we tested one additional case with mdrag value in the CUPID input. As shown in Table 9, the bundle level axially integrated average was calculated to compare the magnitude of the variation, but the magnitude was too small to be considered. The maximum absolute change in the equilibrium quality for the sub-channel was only 0.26% while average equilibrium quality was almost the same, the maximum relative change in the mass flux for

Table 10
Basic T/H properties in bundle 10.

Sub-channel Index	Density (kg/m^3)		Temperature (°C)		Pressure (kPa)	
	ASSERT	CUPID Relative Difference (%)	ASSERT	CUPID Difference	ASSERT	CUPID Difference
1	384.9	10.2	584.6	2.8	84.8	−6.8
2	479.9	−6.7	584.6	2.7	84.9	−6.8
3	623.7	−23.3	584.4	2.4	84.9	−6.8
4	585.7	−18.7	584.4	2.4	84.9	−6.8
5	706.6	−2.9	582.6	−2.9	84.7	−6.8
6	534.7	10.8	584.5	1.6	84.7	−6.8
7	753.0	−4.0	581.7	−2.7	84.8	−6.8
8	520.9	−12.2	584.5	2.6	84.9	−6.8
9	773.5	−6.2	578.7	−0.3	85.0	−6.8
10	562.7	−13.8	584.4	2.7	85.0	−6.8
11	765.0	−7.8	580.5	−0.9	85.0	−6.8
12	766.3	−6.0	580.9	2.0	84.6	−6.8
13	621.1	11.8	584.5	0.4	84.6	−6.8
14	729.7	−16.7	582.4	1.6	84.7	−6.8
15	640.7	7.8	584.5	0.1	84.7	−6.8
16	767.2	−6.2	580.8	2.0	84.8	−6.8
17	669.8	5.0	584.5	−0.3	84.8	−6.8
18	770.2	−3.2	579.7	1.1	84.9	−6.8
19	714.8	−8.1	584.3	0.7	84.9	−6.8
20	758.0	−2.9	582.5	−0.6	85.0	−6.8
21	713.5	−18.4	584.3	1.8	85.1	−6.8
22	772.0	−1.8	578.9	2.8	85.1	−6.8
23	621.5	3.6	584.5	0.8	85.1	−6.8
24	760.5	−7.1	581.6	1.0	85.1	−6.8
25	808.4	−0.6	565.1	1.5	84.5	−6.8
26	800.2	−1.6	568.5	−0.3	84.5	−6.8
27	798.3	−1.9	569.3	−0.1	84.6	−6.8
28	798.1	−0.2	569.4	−1.2	84.7	−6.8
29	786.5	0.9	573.9	−3.1	84.8	−6.8
30	772.5	0.6	579.0	−4.6	84.9	−6.8
31	754.3	−2.9	582.3	−2.4	85.0	−6.8
32	665.3	−0.5	584.5	−2.4	85.1	−6.8
33	588.5	5.1	584.5	−0.5	85.2	−6.8
34	596.8	21.8	584.5	−0.6	85.2	−6.8
Avg.	720.4	−2.9	579.6	−0.2	84.9	−6.7

Table 11
Void fraction in bundle 10.

Sub-channel Index	Void Fraction	
	ASSERT	CUPID Difference (%)
1	0.536	−6.3
2	0.398	4.0
3	0.192	20.3
4	0.246	15.1
5	0.079	4.2
6	0.320	−8.8
7	0.017	5.5
8	0.339	8.5
9	0.000	6.9
10	0.279	10.5
11	0.005	9.0
12	0.001	5.8
13	0.195	−10.7
14	0.047	17.0
15	0.167	−7.2
16	0.001	6.0
17	0.125	−4.7
18	0.001	3.1
19	0.061	8.2
20	0.006	3.4
21	0.063	18.3
22	0.001	0.8
23	0.194	−3.4
24	0.006	7.4
25	0.000	0.1
26	0.000	1.9
27	0.000	2.1
28	0.000	0.7
29	0.000	0.1
30	0.000	1.1
31	0.012	4.2
32	0.131	1.5
33	0.242	−4.1
34	0.230	−18.5
Avg.	0.072	3.1

the sub-channel was only 1.03%. Different from the equilibrium quality, the mass flux was normalized and the relative error was calculated. The Root Mean Square Error (RMSE) for the mass flux was only 0.21%.

4.3. Pressure drop control

The pressure drop difference between the CUPID code and the ASSERT code was about 70–80 kPa. The amount of pressure drop difference could not be ignored considering that the relative portion of the difference was about 25% of the reference pressure drop of the ASSERT code. Of course, this much of pressure drop difference cannot be ignored. Essentially, the pressure drop should be consistent. Therefore, an artificial form loss was given to the CUPID code to fit the pressure drop of the CUPID code to that of the ASSERT code. Overall procedure is shown in Fig. 5. Artificial pressure drop control often occurs in the T/H analysis. Because we are doing numerical simulation, we can have some distance from the real situation which is interpreted in this study with the ASSERT code. The amount of change in artificial form loss can be changed depend on the simulation condition.

4.4. Code to code comparison with the reference model, mesh and artificial form loss

After determining of the reference mesh and model options, we made a comparison between the ASSERT code and the CUPID code. Because of the CUPID code's use the FVM, a geometrical truncation error occurred-any discretization would introduce geometrical truncation error for non-polygonal model. To eliminate the flow area error due to FVM, we reduced the fuel rod radius in the ASSERT analysis to retain the flow area. Because geometrical truncation error appears, the equivalent fuel radius can be found by hand calculation without any change in other dimensions such as rod position. The geometrical truncation error due to pressure tube is ignored.

In the typical high power PHWR channel, the most CHF probable bundle number is known to be bundle 10. Moreover, the sub-channel around the center rod and the sub-channel which has the smallest flow area located at the end of the gravitational force direction in the most outer region are known to be the most CHF probable regions. Thus in this study, final comparison between the ASSERT code and the CUPID code was made in the bundle 10 region. Because the CUPID code uses 2 axial sub-segments for a bundle while the ASSERT code uses 6, we needed to calculate the average of the two codes. The pressure, temperature and density used the sub-channel volume as the weighting function. The enthalpy and equilibrium quality used the sub-channel mass as the weighting function. The mass flux used the flow area for the averaging.

In bundle 10, although the highest power bundles are 6 and 7, still is there a strong heat source, and pressure is sufficiently decreased to generate much steam. For example, the void fraction in sub-channel number 1 reaches almost 50%. As shown in Table 10, the basic properties, namely, temperature and pressure, are slightly different from each other. The pressure difference between sub-

Table 12
Enthalpy, equilibrium quality and mass flux in bundle 10.

Sub-channel Index	Mixture Enthalpy (mj/kg)<		Equilibrium Quality		Normalized Mass Flux	
	ASSERT	CUPID Difference	ASSERT	CUPID Difference (%)	ASSERT	CUPID Relative Difference (%)
1	1.48	−25.0	0.109	−2.0	0.51	27.2
2	1.43	15.8	0.065	1.5	0.60	13.0
3	1.38	49.7	0.024	4.4	0.77	−9.4
4	1.39	40.7	0.033	3.6	0.74	−13.1
5	1.35	−12.6	−0.001	−0.9	1.02	1.6
6	1.41	−13.5	0.047	−1.0	0.68	15.2
7	1.34	−9.9	−0.012	−0.7	1.09	−1.3
8	1.42	27.5	0.051	2.5	0.65	10.0
9	1.32	4.4	−0.027	0.5	1.13	−4.0
10	1.40	32.2	0.039	2.9	0.71	0.9
11	1.33	2.9	−0.018	0.4	1.11	−4.5
12	1.34	17.2	−0.016	1.6	1.13	−7.5
13	1.38	−14.0	0.024	−1.1	0.87	14.5
14	1.35	30.7	−0.006	2.8	1.09	−13.3
15	1.38	−10.8	0.020	−0.8	0.89	14.0
16	1.34	16.8	−0.016	1.6	1.13	−6.0
17	1.37	−7.7	0.014	−0.5	0.93	7.9
18	1.33	9.0	−0.021	0.9	1.18	−5.0
19	1.36	13.8	0.006	1.3	0.99	−1.5
20	1.35	0.2	−0.008	0.2	1.06	2.2
21	1.36	36.3	0.006	3.2	0.98	−11.6
22	1.33	17.0	−0.026	1.6	1.18	−3.2
23	1.38	−3.3	0.024	−0.1	0.85	9.8
24	1.34	13.3	−0.012	1.3	1.12	−6.4
25	1.25	8.8	−0.089	0.9	1.17	−6.1
26	1.27	−0.4	−0.074	0.1	1.15	−3.3
27	1.27	0.9	−0.070	0.2	1.13	−3.0
28	1.27	−5.2	−0.070	−0.3	1.10	−0.8
29	1.30	−15.4	−0.049	−1.2	1.05	0.1
30	1.33	−23.9	−0.025	−1.9	1.01	1.8
31	1.35	−9.8	−0.008	−0.7	0.94	2.5
32	1.37	−15.0	0.015	−1.1	0.80	12.2
33	1.39	−15.7	0.032	−1.2	0.68	22.5
34	1.39	−31.2	0.030	−2.5	0.69	29.3
Avg.	1.34	0.5	−0.017	0.2	6732.2	N/A

channels is actually negligible and finally an approximate 7 kPa difference appeared. For the temperature, the maximum difference of 4.6° was observed at sub-channel 30. Among the basic T/H properties, density had the largest error. Because the void fraction error was sometimes as high as 20%, the density and thus the mass flux could not be accurate. By considering that densities are almost the same in the single phase region of bundle 1 to bundle 7, the density error in bundle 10 came mainly from the void fraction difference, the maximum 20.3% absolute difference at sub-channel 3, as shown in Table 11.

From the point of view of the CHF, we had three factors, pressure, mass flux and equilibrium quality., as shown in Table 12, those 3 parameters were compared. While the pressure difference seemed to be negligible as before, the mass flux difference seemed quite high. But as mentioned, the density error due to sub-channel wise void fraction amplified the mass flux error in bundle 10. The maximum 29.3% mass flux error at sub-channel 34 was obtained from the results analysis along with the maximum 4.4% equilibrium quality error at sub-channel 3. The mixture enthalpy error matched the equilibrium quality error well with respect to the magnitude of error and location.

The average density relative error, temperature and pressure absolute errors between the two codes were 2.9%, 0.2 celsius degrees and 6.7 kPa, respectively. The average mixture enthalpy, void fraction, equilibrium quality and mass flux absolute errors were only 49 kj/kg (0.04% relative to reference ASSERT value), 3.1%, 0.2% and 155 kg/m^{2}s (−2.29% relative to the reference ASSERT value).

5. Discussions and conclusions

This study assessed the effectiveness of the CUPID code in a heavy water channel system. Because the PHWR has a horizontal flow direction while the LWR has a vertifcal flow direction, high pressure drop compared with that in LWR-about 300–400 kPa for design value, heavy water for fluid property although the difference is not that much compared with the light water, the benchmarking of the CUPID code should be done prior to active utilization of the CUPID code. In addition, despite the single phase in the LWR, there is boiling, quite a high equilibrium quality and void fraction in the PHWR core. It was already mentioned that the ASSERT code has various verification and validation results even though those results have not opened one hundred percent. Thus, the benchmarking through the ASSERT code give us further implication. In this sense, it is possible to say that we are benchmarking the ASSERT code V&V experience.

There were several drawbacks in this study. First, the detailed geometrical modeling was omitted, such as bearing pads, spacer grids and end plates, which affect the pressure drop significantly. Moreover, the axial power distribution and radial power distribution were slightly different from the actual core power distribution; we used mid-burnup ring power distribution and cosine shape power distribution for the axial power distribution. In reality the fuel was composed of three regions, namely, pellet, gap and cladding, while the three regions were combined as one fuel region in this study.

One point is that the ASSERT code cannot produce symmetric

results although the geometry and conditions were theoretically symmetric because composing symmetric boundary condition is impossible in the ASSERT code. At the same time the CUPID code used symmetric boundary condition for the x = 0 plane. Thus, this should be taken into account on assessment.

Despite the few weaknesses, from the point of view of CHF prediction, the CUPID code showed us solution of reasonable resolution in the PHWR channel. In the region with a high void fraction, the maximum errors for pressure, temperature and density were 6.8 kPa (sub-channel 11), 4.6 celsius degree (sub-channel 30) and 145 kg/m^3 (sub-channel 3) in bundle 10. The maximum errors for the void fraction, mixture enthalpy, equilibrium quality and mass flux were 20.3% (sub-channel 3), 49.7 kj/kg (sub-channel 3), 4.4% (sub-channel 3) and 1124 kg/m^{2}s (sub-channel 14) in bundle 10.

Note that all cases in this study have y plus over 700. But additional study of approximately 500 y plus around fuel rod wall and pressure tube wall for given k-epsilon tubuelence model was done and it showed that changes of crucial values of equilibrium quality, mass flux and pressure are imaginal. In the future, flow distribution depend on the full modeling can be examined by expanding this computational work will be possible. In addition, works which will be done with the CUPID code in the near future can obtain more credit such as pressure tube deformation research on thermal margin decrement.

Declaration of competing interest

The authors declare that they have no known competing financial interests or personal relationships that could have appeared to influence the work reported in this paper.

Acknowledgements

This work was supported by the National Research Foundation of Korea (NRF) grant funded by the Korea government (Ministry of Science and ICT). (Project No. RS-2022-00155533).

References

[1] Y.F. Rao, Z. Cheng, G.M. Waddington, A. Nava-Dominguez, ASSERT-PV 3.2: advanced subchannel thermal hydraulics code for CANDU fuel bundles, Nucl. Eng. Des. 275 (2014) 69–79.
[2] A. Nava-Dominguez, Y.F. Rao, G.M. Waddington, Assessment of subchannel code ASSERT-PV for flow-distribution predictions, Nucl. Eng. Des. 275 (2014) 122–132.
[3] J.J. Jeong, H.Y. Yoon, I.K. Park, H.K. Cho, The CUPID code development and assessment strategy, NET 42 (6) (2010) 635–655.
[4] H.Y. Yoon, J.R. Lee, I.K. Park, C.H. Song, H.K. Cho, J.J. Jeong, Recent improvements in the CUPID code for a multi-dimensional two-phase flow analysis of nuclear reactor components, NET 42 (6) (2010) 635–655.
[5] J.R. Lee, S.G. Park, H.Y. Yoon, H.T. Kim, J.J. Jeong, Numerical study for CANDU moderator temperature prediction by using the two-phase flow analysis code, CUPID, Ann. Nucl. Energy 59 (2013) 139–148.
[6] S.R. Choi, J.J. Jeong, J.R. Lee, H.Y. Yoon, Numerical investigation of the CANDU moderator thermal-hydraulics using the CUPID code, Prog. Nucl. Energy 85 (2015) 541–547.
[7] S.J. Lee, I.K. Park, H.Y. Yoon, J.W. Kim, Natural circulation analysis considering variable fluid properties with the CUPID code, J. Computat. Fluids Eng. 20 (4) (2015) 14–20.
[8] J.R. Lee, H.Y. Yoon, I.K. Park, S.J. Lee, Y.J. Cho, CUPID Code Manuals, KAERI/TR-6528, 2016.
[9] M.H.A. Piro, F. Wassermann, S. Grundmann, B. Tensuda, S.J. Kim, M. Christon, M. Berndt, M. Nishimura, C. Tropea, Fluid flow investigations within a 37 CANDU fuel bundle supported by magnetic resonance velocimetry and computational fluid dynamics, Int. J. Heat Fluid Flow 66 (2017) 27–42.
[10] Zheng Lu, Computational fluid dynamics investigations of flow through an aged CANDU pressure tube, Appl. Sci. Nucl. Eng. (2021). University of Ontario Institute of Technology, Thesis on Master Degree.
[11] G.G. Lee, D.H. Ahn, H.H. Jin, M.H. Song, J.Y. Jung, Multilevel modeling of diametral creep in pressure tubes of Korean CANDU units, Nucl. Eng. Technol. 53 (2021) 4042–4051.
[12] S.J. Lee, J.H. Lee, B.J. Kim, Improvement of the two-fluid momentum equation using a modified Reynolds stress model for horizontal turbulent bubbly flows, Chem. Eng. Sci. 173 (2017) 208–217.
[13] Avramova Maria, DEVELOPMENT OF AN INNOVATIVE SPACER GRID MODEL UTILIZING COMPUTATIONAL FLUID DYNAMICS WITHIN A SUBCHANNEL ANALYSIS TOOL", College of Engineering, Pennsylvania State University, 2007. Thesis on Doctor of Philosophy.
[14] M.H.A. Piro, F. Wassermann, S. Grundmann, B.W. Leitch, C. Tropea, Progress in on-going experimental and computational fluid dynamics investigations within a CANDU fuel channel, Nucl. Eng. Des. 299 (2015) 184–200.